EPJ Web of Conferences **140**, 06010 (2017) DOI: 10.1051/epjconf/201714006010
Powders & Grains 2017

Jamming Transition: Heptagons, Pentagons, and Discs

Yuanyuan Xu[1,⋆], *Jonathan* Barés[2,⋆⋆] *Yiqiu* Zhao[2,⋆⋆⋆] and *Robert P.* Behringer[2,⋆⋆⋆⋆]

[1] *Taishan College, Shandong University, Jinan, Shandong 250100, China*
[2] *Department of Physics and Center for Nonlinear and Complex Systems, Duke University, Durham, North Carolina 27708, USA*

Abstract.
The jamming behavior of a system composed of discs has been well documented. However, it remains unclear how a granular system consisting of non-spherical particles transitions between unjammed and jammed states. Here, we present compression experiments to study the jamming transition of 2D granular materials composed of photoelastic heptagonal particles and compare these results to data for discs and pentagons. We determine the critical packing fraction of heptagons and make a comparison to discs and pentagons. In the experiment, we subject 618 heptagonal particles to cyclic compression. We track the motion (inlcuding rotations) of the particles, and we measure forces on particles by photoelasticity. We observe a power law relationship between the average contact number (Z) and the pressure (P). Furthermore, we classify the type of contacts by the relative orientation of pairs of contacting particles (creating point-to-face and face-to-face contacts), and we explore the evolution of the contacts during jamming.

1 Introduction

Jamming occurs when materials like foams, glasses and granular materials become mechanically rigid and stable. The jamming transition has become an important research topic in physics and chemistry, and it has a wide range of applications in industrial productions and environmental events. In recent years, many interesting features have been found in systems composed of discs or ellipses [1] [2] [3] [4] [5][6]. Simulations for polygons and other complex shapes have also been carried out [7] [8] [9] [10][11]. We provide an experimental study of more complex particles, pentagons and heptagons, to bridge the gap between simulation and physical experiment. We focus particularly on heptagons, but we make comparision to discs and pentatons.

In this work we focus on a system of heptagons that we compress and decompress via many small steps. The system consists of 618 heptagonal particles in two dimensions. We use photoelastic techniques [1] to measure the system pressure and to study the formation of contacts and force chains. Image processing methods and mathematical criteria are applied to both count the number of contacts and classify the type of the contact. We find the relation between the number of point-to-face contacts and face-to-face contacts, which is crucial to understanding force transmission near jamming.

⋆e-mail: xuyy95@outlook.com
⋆⋆e-mail: jb427@phy.duke.edu
⋆⋆⋆e-mail: yiqiu.zhao@duke.edu
⋆⋆⋆⋆e-mail: bob@phy.duke.edu

2 Experimental setup

The experiments consists of biaxial compression of quasi-2D systems of photoelastic particles. We have three samples: 618 heptagons with side length 6.93 mm and thickness 6.35 mm; 784 pentagons with side length 9.40 mm and thickness 6.35 mm; 895 discs with radius 6.35 mm and thickness 5.56 mm. The inter-particle friction coefficient is 0.7 for discs and 0.9 for pentagons and heptagons. We draw a dot and a bar on the top of each particle in UV-fluorescent ink and these markers give us the position and the orientation of the particle when the system is illuminated with UV light. Figure 1 shows a schematic of the experiment. All particles are randomly placed on a horizontal Plexiglas sheet (38.60 cm × 38.32 cm) lubricated by a thin layer of talcum powder and prepared in a stress-free state initially. Two movable walls (blue arrows) driven by linear motors compress the system quasi-statically via small steps (0.4 mm per step) until the system is in a strongly jammed state. Then, the system is decompressed step by step to the initial packing fraction. After each step, the camera above the container records three types of images (see Fig. 2). From UV light images, we extract the center and the orientation of each particle. We then use the white light images to fine tune the particle positions. The photo-elastic image gives the global pressure using a gradient squared measure[2]. Contacts between particles are detected using the *Shadow Overlap* method devised by Moreau [12] and then the true force-transmitting contacts can be screened out by using the photoelastic image and examining the region around each possible contact [2].

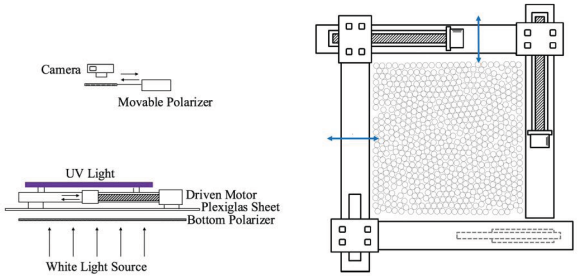

(a) (b)

Figure 1: Schematics of the biaxial compression experiments. (a) Side view of the setup. (b) Top view of the setup.

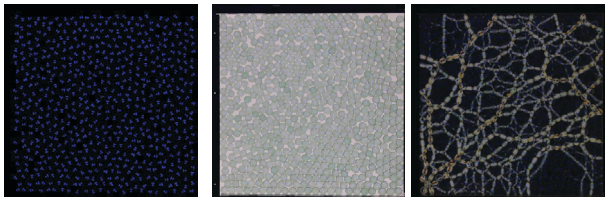

(a) (b) (c)

Figure 2: (a) UV light image: white light is off and UV light is on. (b) White light image: only white light is on. (c) Photo-elastic image: white light is on and the crossed polarizer is moved under the camera.

3 Results

3.1 Critical packing fraction

Figure 3 shows the pressure versus packing fraction for heptagonal particles during one cycle of compression/decompression. There exists a well defined point in the decompression process where there is a sharp transition and we define the packing fraction ϕ_c at this point as the jamming or critical packing fraction. The global pressure, determined by G^2, in decompression is higher than that in the compression for larger ϕ's ($\phi > \phi_c$). We made 20 runs with the same initial packing fraction (see Fig. 4a) and the average value of ϕ_c for heptagonal particles is 0.767. We also carried out similar experiments for discs and pentagons. Figure 4b shows a comparison of the average ϕ_c for heptagons, pentagons, and discs. We find that $\bar{\phi}_c^{Hept} < \bar{\phi}_c^{Pent} < \bar{\phi}_c^{disc}$. As a comparison, Figure 5 presents G^2 vs. packing fraction in pentagon decompression experiments. The inserted panel of Figure 5 shows the scatter of the critical packing fractions. Except perhaps for the first few cycles, there is no systematic variation of ϕ_c with cycle number.

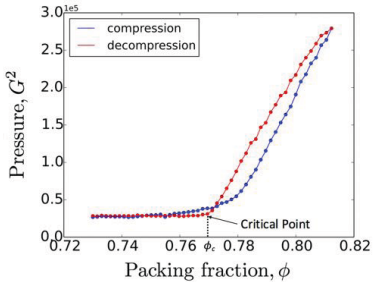

Figure 3: Evolution of the global pressure, measured by G^2, during one cycle. Blue dots are compression process and red dots are decompression process.

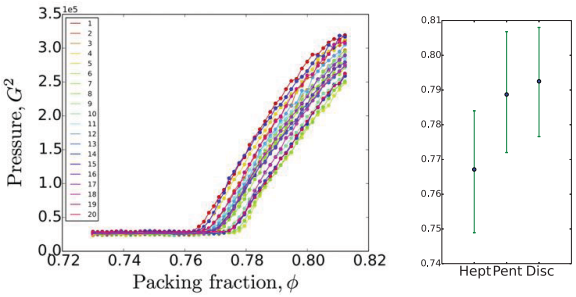

(a) (b)

Figure 4: (a) Results from 20 runs for heptagons starting from the same boundary configuration. Different colors denote different runs. (b) A comparison of the average ϕ_c for the three particle types: 1) 618 heptagons with side length 6.93 mm, 2) 784 pentagons with side length 9.40 mm, and 3) 895 discs with radius 6.35 mm. Note that the blue dot represents the average value and the green bar represents the range of values.

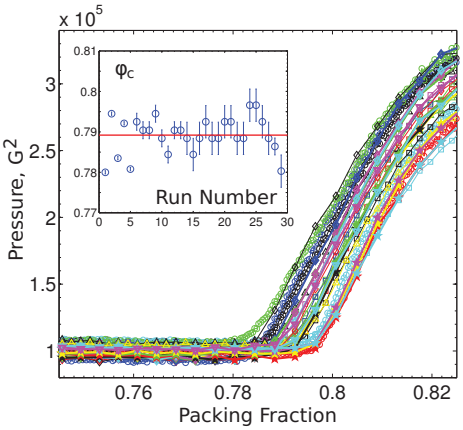

Figure 5: Main panel: results from runs of pentagon decompression starting from same packing fraction. Inserted figure: the value of critical packing fraction detected from each run.

3.2 Contact number

The average contact number Z is computed by counting only the force bearing heptagons, i.e., each particle has at least 2 contacts [3]. Figure 6a shows the evolution of the average contact number during one cycle of compression. We find that the ϕ dependence of Z is qualitatively similar to the ϕ dependence of G^2 (Fig. 3). From a log-log plot of Z vs. G^2 (see Fig. 6b), we observe a power law relationship between the average contact number and the global pressure, i.e., $Z - Z_c \propto (G^2 - G_c^2)^\alpha$. We made 10 runs starting from the same packing fraction and found $\alpha = 0.253$ (standard deviation $\sigma = 0.017$).

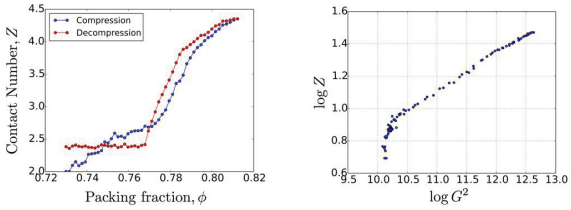

(a) (b)

Figure 6: (a) Average contact number Z vs. packing fraction ϕ. (b) Log-log plot of Z vs. G^2. The data follow a straight line for larger enough values.

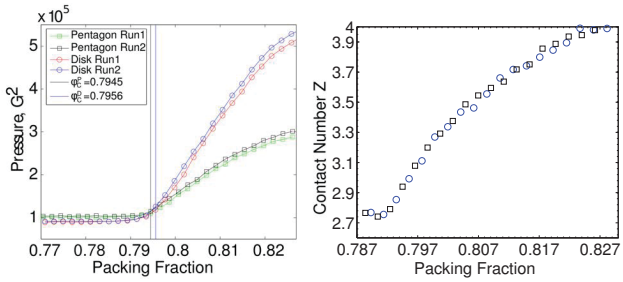

(a) (b)

Figure 7: (a) Runs from discs and pentagons possessing similar critical packing fraction. (b) The average contact number for pentagons (squares) and discs (circles) show qualitatively similar variation with ϕ as for same shape with heptagons. The color indicates same runs as in (a)

For comparison, we also studied the variation of the average contact number during the decompression process for discs and pentagons. To control variables, we choose two runs with similar critical density, one from discs and the other from pentagons. As shown from Figure 7, we see qualitatively similar behaviors for all three kinds of particles: discs, pentagons and heptagons.

3.3 Classification of contact

Previous simulations indicate that strong forces are mainly carried by face-to-face (flat) contacts while weak forces are mostly carried by point-to-face (point) contacts [7]. In order to understand the structure of the contact network, we studied the evolution of the flat and point contacts (see Fig. 8a). Figure 8b shows the number of the point contacts versus the number of the flat contacts and the data points lie close to a straight line.

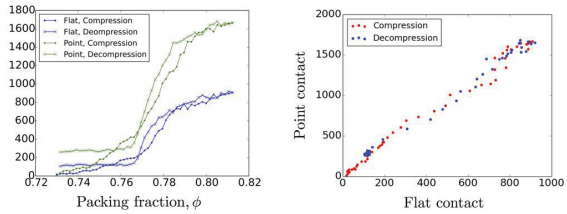

(a) (b)

Figure 8: Data for contact types. (a) Blue curve shows the number of the face-to-face contacts and green curve shows the number of the point-to-face contacts. (b) Number of the point-to-face contacts vs. number of the face-to-face contacts.

We made 10 runs starting from the same packing fraction and the data is fitted by a straight line. From Figure 9, we found that the ratio of the point-to-face contacts to face-to-face contacts is about 1.834 in the compression process and 1.857 in the decompression process.

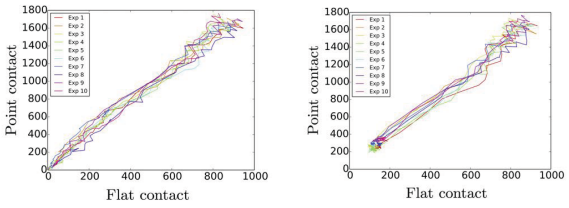

(a) (b)

Figure 9: (a) Compression process: mean slope $k = 1.834$, standard deviation $\delta = 0.090$. (b) Decompression process: mean slope $k = 1.857$, standard deviation $\delta = 0.081$.

The inverse problem of non-spherical photoealstic particles has not been developed. To estimate the role of flat and point contacts in the force network, we calculate the ratio of flat and point contacts for the particles that bear a pressure larger than the system average. The result for a typical heptagon run is presented in Figure 10. All runs of the experiments possess qualitatively similar properties. In this run, the system was compressed during 1 to 50 experimental steps, and decompressed during 51 to 100 experimental steps. The ratio calculated from particles possessing pressure larger than average ($G^2 > average$) remains close to the ratio calculated from the whole system during all the experimental steps, indicating no special role for large force vs small force contacts during heptagon jamming transition.

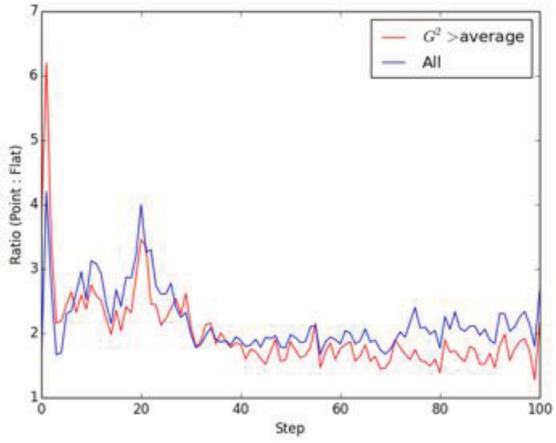

Figure 10: The point (point-to-face) to flat (face-to-face) contact ratio for heptagon particles in a particular run. Step 1 to 50 corresponds to compression process and step 51 to 100 corresponds to decompression process.

4 Conclusions

We present data for the critical packing fraction in the decompression process for pentagons, heptagons, and discs. We observe a power law relationship between the average contact number Z and the global pressure G^2 which follows $Z - Z_c \propto (G^2 - G_c^2)^{0.253}$. In addition, the ratio of the point-to-face contacts to face-to-face contacts is around 1.85. In particular, we find the ratio calculated from particles with pressure larger than average remains the same as the ratio calculated from all particles. However, the inverse problem of non-spherical photoelastic particles should be developed to give a more precise conclusion.

Acknowledgements

This work was supported by NSF grants DMR1206351, and DMS1248071, NASA grant NNX15AD38G, and a grant from the William M. Keck Foundation.

References

[1] T.S. Majmudar, R.P. Behringer, Nature **435**, 1079 (2005)
[2] T. Majmudar, D. University, *Experimental Studies of Two-dimensional Granular Systems Using Grain-scale Contact Force Measurements* (Duke University, 2006), ISBN 9780549109396
[3] T.S. Majmudar, M. Sperl, S. Luding, R.P. Behringer, Phys. Rev. Lett. **98**, 058001 (2007)
[4] S. Farhadi, R.P. Behringer, Physical review letters **112**, 148301 (2014)
[5] S. Farhadi, R.P. Behringer, Phys. Rev. Lett. **112**, 148301 (2014)
[6] C.S. O'Hern, L.E. Silbert, A.J. Liu, S.R. Nagel, Phys. Rev. E **68**, 011306 (2003)
[7] E. Azéma, F. Radjaï, R. Peyroux, G. Saussine, Phys. Rev. E **76**, 011301 (2007)
[8] T. Schilling, S. Pronk, B. Mulder, D. Frenkel, Physical Review E **71**, 036138 (2005)
[9] E. Azéma, F. Radjaï, Physical Review E **81**, 051304 (2010)
[10] Y.L. Duparcmeur, A. Gervois, J.P. Troadec, Journal of Physics: Condensed Matter **7**, 3421 (1995)
[11] F. Alonso-Marroquin, H. Herrmann, S. Luding, Proceedings of IMECE, New Orleans, Loisiana, Nov. 2002, CD: ASME2002-32498 (2002)
[12] G. Saussine, C. Cholet, P. Gautier, F. Dubois, C. Bohatier, J. Moreau, Computer Methods in Applied Mechanics and Engineering **195**, 2841 (2006)